J. Micromech. Microeng. **12** (2002) 948–954 PII: S0960-1317(02)37136-5

Efficient design of micromechanical gyroscopes

Vladislav A Apostolyuk[1], **V J Logeeswaran**[2] **and Francis E H Tay**[2]

[1] Institute of Materials Research and Engineering, Micro- and Nano-Systems Laboratory, 3 Research Link, Singapore 117602
[2] Department of Mechanical Engineering, National University of Singapore, 10 Kent Ridge Crescent, Singapore 119260

E-mail: v-apostol@imre.org.sg, loges@nus.edu.sg and mpetayeh@nus.edu.sg

Received 17 May 2002, in final form 5 September 2002
Published 17 October 2002
Online at stacks.iop.org/JMM/12/948

Abstract
We consider a general approach to the analysis of the dynamics and errors of different types of micromechanical vibratory gyroscopes, as well as calculation of their performances for application in the design of such gyroscopes. Specifically, we investigate and analyse the dynamics and errors of single-mass gyroscopes, for both translational and rotational movement of the sensitive element. Based on the generalized motion equations, we derive and analyse analytical dependences for basic errors, such as scale factor nonlinearity, bias from misalignment between elastic and measurement axes, and bias from vibrations and dynamic error caused by harmonic angular rate. As a result of dynamics and errors analysis, formulae for the calculation of the main performances are derived, as well as optimal sensitive element design methodologies.

1. Introduction

Fabrication technologies for microcomponents, microsensors, micromachines and microelectromechanical systems (MEMS) are being rapidly developed, and represent a major research effort worldwide. There are many techniques currently being utilized in the production of different types of MEMS, including inertial microsensors, which have made it possible to fabricate MEMS in high volumes at low individual cost. Micromechanical vibratory gyroscopes or angular rate sensors have a large potential for different types of applications as primary information sensors for control and navigation systems. They represent an important inertial technology because other gyroscopes, such as solid-state gyroscopes, laser ring gyroscopes and fibre optic gyroscopes, do not allow for miniaturization. MEMS sensors are commonly accepted as low performance and low cost sensors. Nevertheless, recent applications have resulted in the need for sensors with improved performances. High performances can be achieved by means of improved sensitive element and circuit design.

One of the ways to improve performances of micromechanical vibratory gyroscopes is to analyse their dynamics and errors in order to find efficient design methodologies. Mathematical models of symmetrical (without decoupling frames) sensitive elements with translational movement of a proof mass, applicable to the analysis of micromechanical gyroscopes as well as control principles, were considered in [1–3]. Dynamics and errors of gimbaled and tuning-fork micromechanical gyroscopes were considered in [5–7]. Dynamics and errors of translation micromechanical gyroscopes with decoupling frames were studied in [8, 9]. Some calculations of performances for micromechanical gyroscopes with translational oscillations of a proof mass were considered in [10, 11]. Nevertheless, no analytical approaches to design have been developed, which leads to the need in numerous simulations and experimental researches to try to find appropriate designs for sensitive elements.

In this paper, we consider a general approach to the analysis of the dynamics and errors of different types of micromechanical vibratory gyroscopes as well as the calculation of their performances for application in the design of such gyroscopes.

2. Operation principle and motion equations

In most micromechanical vibratory gyroscopes, the sensitive element can be represented as an inertia element and elastic

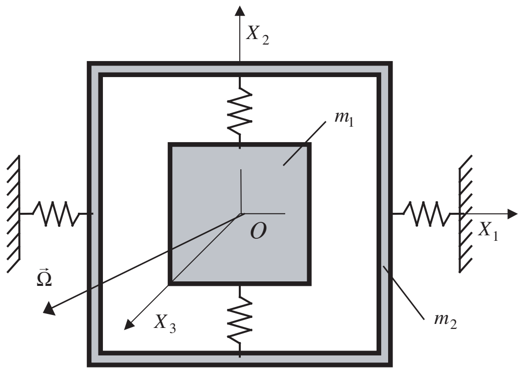

Figure 1. Sensitive element of a micromechanical vibratory gyroscope.

suspension with two prevalent degrees of freedom. The sensitive element is driven to oscillate at one of its modes with prescribed amplitude. When the sensitive element rotates about a particular fixed-body axis, the resulting micromechanical force causes the proof mass to be excited in a different mode. It is obvious that information about the angular rate is contained in these different oscillations. Hereafter, excited oscillations are referred to as primary oscillations and oscillations caused by angular rate are referred to as secondary oscillations.

In general, it is possible to design gyroscopes with different types of primary and secondary oscillations. For example, a combination of translation as primary oscillations and rotation as secondary oscillations was implemented in tuning-fork gyroscopes. However, it is typically more convenient for single-mass gyroscopes to be implemented with the same type of primary and secondary oscillations.

The dynamics of a sensitive element of micromechanical gyroscopes can be entirely described by a set of parameters as follows: ω_{01} and ω_{02} are the natural frequencies of primary and secondary oscillations; ζ_1 and ζ_2 are the relative damping factors; ω is the operating (driving) frequency. Natural frequencies and damping factors entirely determine the structural parameters of the sensitive element, such as mass, length of springs and vacuum level among others, for any achievable fabrication process. On the other hand, characteristics such as measurement range, sensitivity, resolution, bias and bandwidth are the subject of sensitive element design process. In this paper, we determine dependences and rules that can allow us to obtain design parameters and technology tolerances on the basis of final performance requirements.

Let us introduce the right-handed orthogonal and normalized reference basis in which primary oscillations are excited along the first axis, secondary oscillations occur along the second axis and, therefore, the third axis is the sensitive axis (see figure 1).

Assuming that the reference basis rotates with an angular rate, of which the vector is $\vec{\Omega} = \{0, 0, \Omega_3\}$, generalized equations of motion of a single-mass sensitive element, with translation of both primary and secondary oscillations, can be presented in the form:

$$\begin{cases} \ddot{x}_1 + 2\zeta_1\omega_{01}\dot{x}_1 + \left(\omega_{01}^2 - d_1\Omega_3^2\right)x_1 + g_1\Omega_3\dot{x}_2 = q_1(t), \\ \ddot{x}_2 + 2\zeta_2\omega_{02}\dot{x}_2 + \left(\omega_{02}^2 - d_2\Omega_3^2\right)x_2 - g_2\Omega_3\dot{x}_1 = q_2(t). \end{cases} \tag{1}$$

Table 1. Dimensionless inertia parameters.

	Translational	Rotational
d_1	1	$(I_{13} + I_{23} - I_{12} - I_{22})/(I_{11} + I_{21})$
d_2	1	$(I_{13} - I_{11})/I_{12}$
g_1	$2m_1/(m_1 + m_2)$	$(I_{12} + I_{11} - I_{13})/(I_{11} + I_{21})$
g_2	2	$(I_{12} + I_{11} - I_{13})/I_{12}$

Here $q_i(t)$ represents either translation or angular acceleration about the corresponding axis that are caused by external forces or torques, and x_i represents either translation or angular displacements of masses. The factors introduced in equation (1) are explained in table 1.

By means of equations (1) we can study the dynamics of both translational and rotational sensitive elements. In table 1, all moments of inertia are presented in the form I_{ij} where the first index refers to the part of the sensitive element (1 is the central mass, 2 is the frame) while the second index refers to the axis; m_1 is the mass of the central proof mass and m_2 is the mass of the frame. One should note that, in case of a sensitive element without an additional frame, $m_2 = 0$. All parameters of inertia presented in table 1 are subjected to the design process. Let us note that the rotational sensitive elements are more amenable to optimization [12].

3. Primary and secondary amplitudes and phases

Assuming an open-loop operation of the gyroscope and zero phase displacement for excitation force, we can represent the right-hand part of equation (1) as follows:

$$q_1(t) = \mathrm{Re}\{q_1\,\mathrm{e}^{\mathrm{i}\omega t}\}, \qquad q_2(t) = 0. \tag{2}$$

We can also represent our generalized variables as

$$\begin{aligned} x_1(t) &= \mathrm{Re}\{\bar{A}_1\,\mathrm{e}^{\mathrm{i}\omega t}\}, & \bar{A}_1 &= A_1\,\mathrm{e}^{\mathrm{i}\varphi_1}, \\ x_2(t) &= \mathrm{Re}\{\bar{A}_2\,\mathrm{e}^{\mathrm{i}\omega t}\}, & \bar{A}_2 &= A_2\,\mathrm{e}^{\mathrm{i}\varphi_2}, \end{aligned} \tag{3}$$

where A_1 and A_2 are the amplitudes and φ_1 and φ_2 are the phases of the primary and secondary oscillations, respectively. Using equations (2) and (3), a complex solution of equations (1) can be obtained:

$$\begin{aligned} \bar{A}_1 &= \frac{q_1\left(\omega_{02}^2 - d_2\Omega_3^2 - \omega^2 + 2\zeta_2\omega_{02}\mathrm{i}\omega\right)}{\bar{\Delta}}, \\ \bar{A}_2 &= \frac{g_2 q_1 \mathrm{i}\omega}{\bar{\Delta}}\Omega_3, \\ \bar{\Delta} &= \left(\omega_{01}^2 - d_1\Omega_3^2 - \omega^2\right)\left(\omega_{02}^2 - d_2\Omega_3^2 - \omega^2\right) \\ &\quad - \omega^2\left(4\zeta_1\zeta_2\omega_{01}\omega_{02} + g_1g_2\Omega_3^2\right) \\ &\quad + 2\mathrm{i}\omega\left[\omega_{01}\zeta_1\left(\omega_{02}^2 - d_2\Omega_3^2 - \omega^2\right)\right. \\ &\quad \left. + \omega_{02}\zeta_2\left(\omega_{01}^2 - d_1\Omega_3^2 - \omega^2\right)\right]. \end{aligned} \tag{4}$$

From equation (1), we can easily obtain real amplitudes of the primary and secondary oscillations

$$A_1 = \frac{q_1\sqrt{\left(\omega_{02}^2 - d_2\Omega_3^2 - \omega^2\right)^2 + 4\omega_{02}^2\zeta_2^2\omega^2}}{\Delta_0},$$

$$A_2 = \frac{g_2 q_1 \omega}{\Delta_0}\Omega_3,$$

$$\Delta_0^2 = \left[\left(\omega_{01}^2 - d_1\Omega_3^2 - \omega^2\right)\left(\omega_{02}^2 - d_2\Omega_3^2 - \omega^2\right) - \omega^2\left(4\zeta_1\zeta_2\omega_{01}\omega_{02} + g_1g_2\Omega_3^2\right)\right]^2 + 4\omega^2\left[\omega_{01}\zeta_1\left(\omega_{02}^2 - d_2\Omega_3^2 - \omega^2\right) + \omega_{02}\zeta_2\left(\omega_{01}^2 - d_1\Omega_3^2 - \omega^2\right)\right]^2 \quad (5)$$

and also their phases given by

$$\mathrm{tg}(\varphi_1) = \frac{2\omega\left[\left(\omega_{02}^2 - d_2\Omega_3^2 - \omega^2\right)b_1 + \omega_{02}\zeta_2 b_2\right]}{\left(\omega_{02}^2 - d_2\Omega_3^2 - \omega^2\right)b_2 - 4\omega_{02}\zeta_2\omega^2 b_1},$$

$$\mathrm{tg}(\varphi_2) = \left(\left(\omega_{01}^2 - d_1\Omega_3^2 - \omega^2\right)\left(\omega_{02}^2 - d_2\Omega_3^2 - \omega^2\right) - \omega^2\left(4\zeta_1\zeta_2\omega_{01}\omega_{02} + g_1g_2\Omega_3^2\right)\right) \Big/ 2\omega\left[\omega_{01}\zeta_1\left(\omega_{02}^2 - d_2\Omega_3^2 - \omega^2\right) + \omega_{02}\zeta_2\left(\omega_{01}^2 - d_1\Omega_3^2 - \omega^2\right)\right],$$

$$b_1 = \omega_{01}\zeta_1\left(\omega_{02}^2 - d_2\Omega_3^2 - \omega^2\right) + \omega_{02}\zeta_2\left(\omega_{01}^2 - d_1\Omega_3^2 - \omega^2\right),$$

$$b_2 = \left(\omega_{01}^2 - d_1\Omega_3^2 - \omega^2\right)\left(\omega_{02}^2 - d_2\Omega_3^2 - \omega^2\right) - \omega^2\left(4\zeta_1\zeta_2\omega_{01}\omega_{02} + g_1g_2\Omega_3^2\right). \quad (6)$$

Using formulae (5) and (6) to obtain the amplitudes and phases respectively, we can determine the sensitivity of single-mass micromechanical vibratory gyroscopes.

4. Sensitivity and linearity

As follows from equation (5), the amplitude of secondary oscillations depends on the angular rate. Let us represent this amplitude by dimensionless variables by means of the following substitution

$$\omega_{01} = \omega_0, \qquad \omega_{02} = \omega_0\delta\omega_0, \qquad \omega = \omega_0\delta\omega, \qquad \Omega_3 = \omega_0\delta\Omega, \quad (7)$$

as a function of new dimensionless variable amplitude given by

$$A_2 = \frac{g_2 q_1 \delta\omega}{\omega_0^2\Delta}\delta\Omega,$$

$$\Delta^2 = \left[\left(\delta\omega_0^2 - d_2\delta\Omega^2 - \delta\omega^2\right)(1 - d_1\delta\Omega^2 - \delta\omega^2) - \delta\omega^2(4\delta\omega_0\zeta_1\zeta_2 + g_1g_2\delta\Omega^2)\right]^2 + 4\delta\omega^2\left[\delta\omega_0\zeta_2(1 - d_1\delta\Omega^2 - \delta\omega^2) + \zeta_1\left(\delta\omega_0^2 - d_2\delta\Omega^2 - \delta\omega^2\right)\right]^2. \quad (8)$$

Note that no assumption has been made about the value of the angular rate. It is obvious that the relationship between the amplitude of the secondary oscillations and the angular rate is not linear. However, for the best performance this dependence has to be linear. The sensitivity can be taken as a tangent at the origin to the curve that is presented by dependence (8). In this case, sensitivity for the relative angular rate $\delta\Omega$ is given by

$$C_\Omega = \frac{g_2 q_1 \delta\omega}{\omega_0^3\sqrt{\left(\left(\delta\omega_0^2 - \delta\omega^2\right)^2 + 4\delta\omega_0^2\delta\omega^2\zeta_2^2\right)\left((1 - \delta\omega^2)^2 + 4\delta\omega^2\zeta_1^2\right)}}, \quad (9)$$

where $A_{20} = C_\Omega\Omega$ is the desirable output as compared with A_2. The dependence of the sensitivity on the natural frequency ratio $\delta\omega_0$ for different drive frequencies $\delta\omega$ is shown in figure 2.

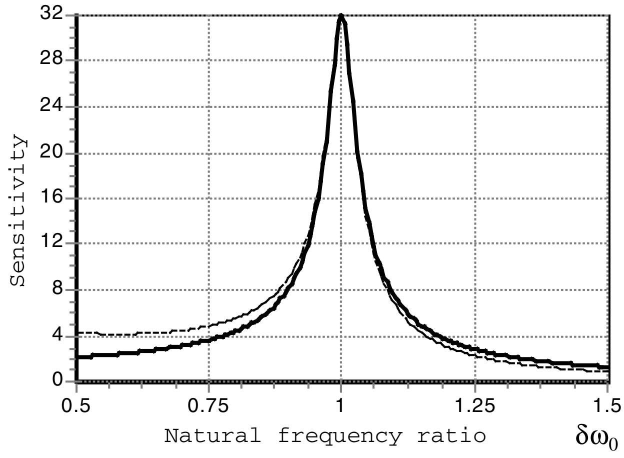

Figure 2. Sensitivity as a function of natural frequency ratio $\delta\omega_0$: the thick curve corresponds to $\delta\omega = 1$, and the thin curve corresponds to $\delta\omega = \delta\omega_0$. The simulation data are: $\omega_0 = 5000\ \mathrm{s}^{-1}$, $\zeta_1 = \zeta_2 = 0.025$, $q_1 = 1\ \mathrm{m\ s}^{-2}$.

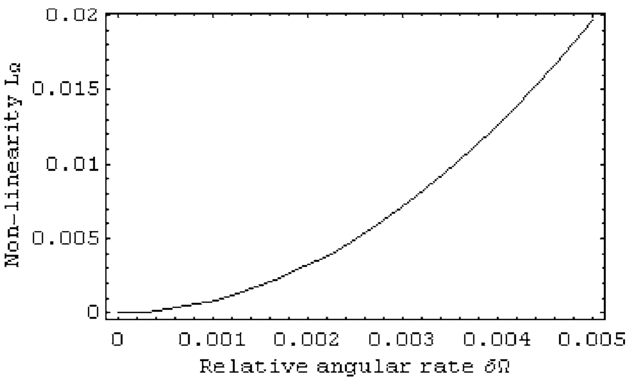

Figure 3. Nonlinearity as a function of the relative angular rate. The simulation data are: $\zeta_1 = \zeta_2 = 0.025$, $g_1 = 1$, $g_2 = 2$, $d_1 = 1$.

Analysis of figure 2 shows that the greatest sensitivity is achievable only if natural frequencies are equal and excitation occurs on the eigenfrequency of primary oscillations. Moreover, considering equation (9) it is obvious that for better sensitivity the natural frequency of primary oscillations ω_0 has to be as low as possible. However, since sensitivity is not the only requirement for the angular rate sensor, exact matching of the natural frequencies usually is not the best choice. On the other hand, this leads us to the nonlinear angular rate transformation. Let us introduce a nonlinearity dimensionless factor as

$$L_\Omega = 1 - \frac{A_2}{A_{20}}.$$

The relationship between L_Ω and the angular rate $\delta\Omega$ is shown in figure 3. For given small values of nonlinearity L_Ω (0–0.05) we can obtain following the approximate formula for the corresponding relative angular rate

$$\delta\Omega^* = \left\{L_\Omega\left[\left(\delta\omega_0^2 - \delta\omega^2\right)^2 + 4\delta\omega_0^2\delta\omega^2\zeta_2^2\right]\left[(1 - \delta\omega^2)^2 + 4\delta\omega^2\zeta_1^2\right] \Big/ \left\{(\delta\omega^2 - 1)D_0 + 4\delta\omega^2\left[g_1g_2\delta\omega_0\delta\omega^2\zeta_1\zeta_2 - d_2\zeta_1^2\left(\delta\omega_0^2 - \delta\omega^2\right)\right]\right\}\right\}^{\frac{1}{2}},$$

$$D_0 = \left(\delta\omega_0^2 - \delta\omega^2\right)\left(d_2 + d_1\delta\omega_0^2 - (d_2 + d_1 - g_1 g_2)\,\delta\omega^2\right) + 4d_1\delta\omega_0^2\delta\omega^2\zeta_2^2. \qquad (10)$$

Assuming an acceptable value for the nonlinearity L_Ω and a required measurement range of the angular rate $\Omega_{\max}$, taking into consideration $\delta\Omega^*$ from equation (10) and substitutions (7), we can calculate the minimal value for the natural frequency of primary oscillations

$$\omega_{0_{\min}} = \frac{\Omega_{\max}}{\delta\Omega^*}. \qquad (11)$$

For example, if $L_\Omega = 0.01$ and $\Omega_{\max} = 1.0\,\mathrm{s}^{-1}$ then the minimal value for the natural frequency of primary oscillations will be $\omega_0 \approx 45$ Hz. Such a low value for the frequency means that the lower limit can be determined in fact by other factors, but nevertheless there is no reason to make it higher than is really necessary.

5. Resolution

The formulae for calculating the resolution of the single-mass micromechanical vibratory gyroscope can be obtained by means of given minimal capacity changes, which the device is capable of detecting. Let us denote this minimal change as $\Delta C_{\min}$. If capacitance C is a function of proof mass displacement δ, then we can write

$$C(\delta) = C(0) + \frac{\mathrm{d}C(0)}{\mathrm{d}\delta}\delta + O(\delta^2).$$

For the small displacements, which are true for the secondary oscillations, we can neglect by $O(\delta^2)$ terms and the capacity change will be given as

$$\Delta C(\delta) = C(\delta) - C(0) \approx \frac{\mathrm{d}C(0)}{\mathrm{d}\delta}\delta.$$

In the case of differential measurements, which are quite commonly accepted in capacitance measurements, the resulting capacitance change is produced by the subtraction of two separately measured capacitances C_1 and C_2 as follows:

$$\Delta C(\delta) = C_1(\delta) - C_2(\delta) \approx 2\frac{\mathrm{d}C(0)}{\mathrm{d}\delta}\delta. \qquad (12)$$

For example, the change in capacity of two parallel conductive plates caused by displacements of the proof mass in the case of differential measurement (12) can be calculated by the following formula

$$\Delta C = \frac{\varepsilon\varepsilon_0 S}{\delta_0 - \delta} - \frac{\varepsilon\varepsilon_0 S}{\delta_0 + \delta} \approx 2\frac{\varepsilon\varepsilon_0 S}{\delta_0^2}\delta.$$

Here, δ_0 is the base gap between the electrodes, δ is the displacement of the electrodes, S is the overlapped area, ε is the relative dielectric constant of the proof mass environment and ε_0 is the absolute dielectric constant of vacuum. The shift of the electrodes caused by changes of the angular rate $\Delta\Omega$ is given by

$$\delta = r_0 C_\Omega \Delta\Omega \qquad (13)$$

where C_Ω is determined by equation (9), r_0 is the distance from the rotation axis to the centre of the electrode for the rotary sensitive element and unity for the translational sensitive element. Thus, comparing equations (12) and (13), we can obtain the resolution of a single-mass micromechanical vibratory gyroscope that is given by

$$\Delta\Omega_{\min} = \frac{\Delta C_{\min}\omega_0^3\sqrt{\left(\left(\delta\omega_0^2 - \delta\omega^2\right)^2 + 4\delta\omega_0^2\delta\omega^2\zeta_2^2\right)\left((1 - \delta\omega^2)^2 + 4\delta\omega^2\zeta_1^2\right)}}{2\frac{dC(0)}{d\delta}r_0 g_2 q_1\delta\omega}. \qquad (14)$$

Note that formula (14) represents the resolution with a capacitive differential readout. However, the same procedure can be applied to any readout principle. The best resolution corresponds to a minimal $\Delta\Omega_{\min}$.

6. Bias

Bias in micromechanical gyroscopes can be the result of many different factors. Let us consider sources of bias concerned with the sensitive element and its dynamics. One of these is vibration at the drive frequency. The interference of vibrations at other frequencies can be filtered. It is obvious that, for the translational gyroscopes, only translational vibration will have an effect, and for rotational gyroscopes only angular vibrations will be relevant. Therefore, in the case of vibrations at drive frequency, the motion equations of the sensitive element will be

$$\begin{cases} \ddot{x}_1 + 2\zeta_1\omega_{01}\dot{x}_1 + \left(\omega_{01}^2 - d_1\Omega_3^2\right)x_1 + g_1\Omega_3\dot{x}_2 = q_1(t) + w_1(t), \\ \ddot{x}_2 + 2\zeta_2\omega_{02}\dot{x}_2 + \left(\omega_{02}^2 - d_2\Omega_3^2\right)x_2 - g_2\Omega_3\dot{x}_1 = w_2(t). \end{cases} \qquad (15)$$

Here $w_1(t)$ and $w_2(t)$ are components of the acceleration vector that represents the motion of the base reference system. By representing the vibrations as $w_i = w_{i0}\cos(\omega t)$, we can obtain the solution of the amplitude of secondary oscillations in dimensionless form

$$A_{W2} = \frac{g_2 q_1\delta\omega\delta\Omega + \sqrt{w_{20}^2(1 - \delta\Omega^2 - \delta\omega^2)^2 + \delta\omega^2(2\zeta_1 w_{20} + g_2\delta\Omega w_{10})^2}}{\omega_0^2\Delta}. \qquad (16)$$

If we denote the amplitude without vibrations as A_{10}, which is given by equation (8), then the relative error caused by vibration at drive frequency is given by

$$\delta A_W = \frac{A_{W2} - A_{10}}{A_{10}} = \frac{\sqrt{w_{20}^2(1 - d_1\delta\Omega^2 - \delta\omega^2)^2 + \delta\omega^2(2\zeta_1 w_{20} + g_2\delta\Omega w_{10})^2}}{g_2 q_1\delta\omega\delta\Omega}. \qquad (17)$$

Let us note that the error arising from vibration does not depend on the ratio between the natural frequencies but depends on the relative drive frequency. This dependency is shown in figure 4.

It can easily be proven that the minimal value for this error achievable at driving frequency is a solution of the following equation

$$1 - \delta\omega^2 - d_2\delta\Omega^2 = 0 \Rightarrow \delta\omega = \sqrt{1 - d_2\delta\Omega^2} \approx 1. \qquad (18)$$

This result also ensures that it is preferable to drive the primary oscillations at their resonance.

Another source of bias is a misalignment between elastic and readout axes. This is most typical for the translation

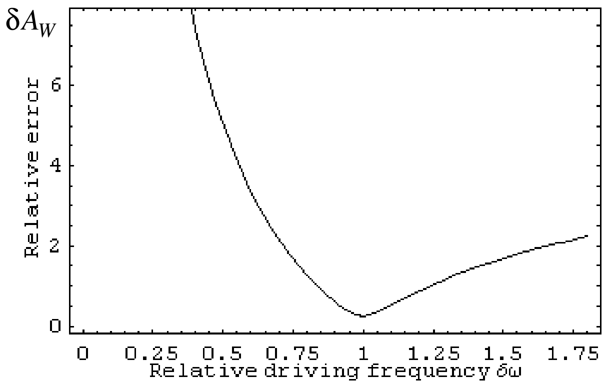

Figure 4. Typical error from vibrations as a function of relative driving frequency. The simulation data are: $\zeta_1 = \zeta_2 = 0.025$, $g_1 = 1$, $g_2 = 2$, $d_1 = 1$, $q_1 = w_1 = w_2 = 1$ m s^{-2}, $\delta\Omega = 10^{-4}$.

sensitive elements. The linearized motion equations in this case will be as follows

$$\begin{cases} \ddot{x}_1 + 2\zeta_1\omega_{01}\dot{x}_1 + \left(\omega_{01}^2 - d_1\Omega^2\right)x_1 + g_1\Omega\dot{x}_2 \\ -2\theta\Delta\omega_1^2 x_2 = q_1(t), \\ \ddot{x}_2 + 2\zeta_2\omega_{02}\dot{x}_2 + \left(\omega_{02}^2 - d_2\Omega^2\right)x_2 - g_2\Omega\dot{x}_1 \\ +2\theta\Delta\omega_2^2 x_1 = 0. \end{cases} \tag{19}$$

Here θ is the misalignment angle, $\Delta\omega_2^2 = (k_2 - k_1)/2M_2$, $\Delta\omega_1^2 = (k_1 - k_2)/2M_1$, where k_1 and k_2 are stiffness, corresponding to primary and secondary oscillations respectively, M_1 and M_2 are inertia factors (for translational motion $M_1 = m_1 + m_2$, $M_2 = m_1$, and for rotational motion $M_1 = I_{11}$, $M_2 = I_{22}$). The amplitude of the secondary oscillations in this case will be

$$\begin{aligned} A_2 &= \frac{q_1\sqrt{g_2^2\delta\omega^2\delta\Omega^2 + 4\theta^2\delta\Delta\omega_2^4}}{\omega_0^2\Delta_\theta}, \\ \Delta_\theta^2 &= \left[\left(\delta\omega_0^2 - d_2\delta\Omega^2 - \delta\omega^2\right)\left(1 - d_1\delta\Omega^2 - \delta\omega^2\right)\right. \\ &\quad \left. - \delta\omega^2(4\delta\omega_0\zeta_1\zeta_2 + g_1g_2\delta\Omega^2)\right]^2 \\ &\quad + 4\delta\omega^2\left[\delta\omega_0\zeta_2(1 - d_1\delta\Omega^2 - \delta\omega^2)\right. \\ &\quad + \zeta_1\left(\delta\omega_0^2 - d_2\delta\Omega^2 - \delta\omega^2\right) \\ &\quad \left. - 2\delta\Omega\theta\left(\delta\Delta\omega_1^2 + \delta\Delta\omega_2^2\right)\right]^2. \end{aligned} \tag{20}$$

It is obvious that if $\theta = 0$ then there is no error arising from misalignment. Moreover, this error will also be absent in the following case

$$\Delta\omega_2^2 = \frac{k_1 - k_2}{2m_1} = 0 \Rightarrow k_1 = k_2. \tag{21}$$

Here k_i are the stiffness factors of the elastic suspension and m_1 is the effective mass of secondary oscillations. In addition, we can represent the amplitude (20) as a sum of two components, namely, one arising from the angular rate and the other caused by misalignment

$$A_2 \approx A_{20} + A_{\theta 2}.$$

In this case, we can determine the relative error from such misalignment as

$$\delta A_\theta = \frac{A_\theta}{A_{20}} = \frac{\theta^2\delta\Delta\omega_2^4}{g_2\delta\omega^2\delta\Omega^2}, \qquad (\Omega \neq 0). \tag{22}$$

On the other hand, we can find an acceptable tolerance for the misalignment θ_{max} with respect to the given acceptable relative bias $\delta\Omega_{max}$ and under the condition of no rotation

$$\theta_{max} = \frac{\delta\Omega_{max}\delta\omega}{\delta\Delta\omega_2^2}. \tag{23}$$

Formula (23) also gives us an angle of misalignment if bias is known. This value can also be used for algorithmic bias compensation. If we can obtain information from other sources of primary information then it is also possible to use dependence (17) for bias compensation.

7. Dynamic error and bandwidth

Let us consider movement of the sensitive element on a basis that rotates with harmonic angular rate

$$\Omega = \Omega_0\cos(\lambda t) = \mathrm{Re}\{\Omega_0\,\mathrm{e}^{\mathrm{i}\lambda t}\}.$$

Taking into account that the frequency of angular rate is small compared to the operation frequency, the corresponding motion equations of the sensitive element in this case are given by

$$\begin{cases} \ddot{x}_1 + 2\zeta_1\omega_{01}\dot{x}_1 + \left(\omega_{01}^2 - d_1\Omega^2\right)x_1 = q_1\cos(\omega t) - g_1\Omega\dot{x}_2 \\ -d_3\dot{\Omega}x_2, \qquad (24a) \\ \ddot{x}_2 + 2\zeta_2\omega_{02}\dot{x}_2 + (\omega_{02}^2 - d_2\Omega^2)x_2 = g_2\Omega\dot{x}_1 + \dot{\Omega}x_1. \qquad (24b) \end{cases}$$

Here d_3 is the constant factor that depends on inertia parameters of the sensitive element. When the amplitude of the angular rate is small ($\Omega_0 \ll \omega_{01}$) and frequency λ of the harmonic angular rate is small in comparison with the natural frequency ω_{01}, we can neglect the right-hand terms in equation (24*a*) except for the excitation term. In addition, centrifugal accelerations in this case are small and hence the equations reduce to

$$\begin{cases} \ddot{x}_1 + 2\zeta_1\omega_{01}\dot{x}_1 + \omega_{01}^2x_1 = q_1\cos(\omega t), \qquad (25a) \\ \ddot{x}_2 + 2\zeta_2\omega_{02}\dot{x}_2 + \omega_{02}^2x_2 = g_2\Omega\dot{x}_1 + \dot{\Omega}x_1. \qquad (25b) \end{cases}$$

The partial solution of equation (25*a*) is given by the following $x_1(t) = \mathrm{Re}\{\bar{A}_1\,\mathrm{e}^{\mathrm{i}\omega t}\} = \mathrm{Re}\{A_1\,\mathrm{e}^{\mathrm{i}(\omega t + \varphi_1)}\}$,

$$A_1 = \frac{q_1}{\omega_0^2\sqrt{(1 - \delta\omega^2)^2 + 4\zeta_1^2\delta\omega^2}}, \qquad \mathrm{tg}(\varphi_1) = -\frac{2\zeta_1\delta\omega}{1 - \delta\omega^2}.$$

Then the right-hand side of equation (25*b*) will be

$$-\frac{\Omega_0}{2}\mathrm{Im}\{\bar{A}_1(g_2\omega + \lambda)\mathrm{e}^{\mathrm{i}f_1t} + \bar{A}_1(g_2\omega - \lambda)\mathrm{e}^{\mathrm{i}f_2t}\},$$
$$f_{1,2} = \omega \pm \lambda.$$

The partial solution of equation (25) for the secondary oscillations x_1 yields a solution given by a sum of two oscillations with frequencies $f_{1,2} = \omega \pm \lambda$

$$x_1(t) = \mathrm{Im}\{\bar{A}_{11}\,\mathrm{e}^{\mathrm{i}f_1t} + \bar{A}_{12}\,\mathrm{e}^{\mathrm{i}f_2t}\}.$$

After substitution of the supposed solution in equation (25*a*) we can find complex amplitudes of secondary oscillations

$$\begin{aligned} \bar{A}_{11,12} &= -\Omega_0q_1(g_2\delta\omega \pm \delta\lambda)\big/2\omega_0^3\left[\delta\omega_0^2 - (\delta\omega \pm \delta\lambda)^2\right. \\ &\quad \left. + 2\zeta_2\delta\omega_0\mathrm{i}(\delta\omega \pm \delta\lambda)\right][1 - \delta\omega^2 + 2\zeta_1\mathrm{i}\delta\omega], \end{aligned}$$

where $\delta\lambda = \lambda/\omega_0$ is the relative frequency of the angular rate. Transition to real amplitude and phase gives us

$$A_{11,12} = \frac{\Omega_0 q_1 (g_2 \delta\omega \pm \delta\lambda)}{2\omega_0^3 \sqrt{\{[\delta\omega_0^2 - (\delta\omega \pm \delta\lambda)^2]^2 + 4\zeta_2^2 \delta\omega_0^2 (\delta\omega \pm \delta\lambda)^2\}\{(1-\delta\omega^2)^2 + 4\zeta_1^2 \delta\omega^2\}}}.$$

Hence, the partial solution for the secondary oscillations is given by

$$x_1(t) = A_{11} \sin[(\omega+\lambda)t + \varphi_{11}] + A_{12} \sin[(\omega-\lambda)t + \varphi_{12}]. \tag{26}$$

Here the phase shifts $\varphi_{11,12}$ are determined from the following expressions

$$\mathrm{tg}(\varphi_{11}) = 2\frac{\delta\omega\zeta_1\left(\delta\omega_0^2 - (\delta\lambda+\delta\omega)^2\right) + \delta\omega_0\zeta_2(1-\delta\omega^2)(\delta\omega+\delta\lambda)}{4\delta\omega_0\delta\omega\zeta_1\zeta_2(\delta\lambda+\delta\omega) - (1-\delta\omega^2)(\delta\omega_0^2 - (\delta\omega+\delta\lambda)^2)},$$

$$\mathrm{tg}(\varphi_{12}) = 2\frac{\delta\omega\zeta_1\left(\delta\omega_0^2 - (\delta\omega-\delta\lambda)^2\right) + \delta\omega_0\zeta_2(1-\delta\omega^2)(\delta\omega-\delta\lambda)}{4\delta\omega_0\delta\omega\zeta_1\zeta_2(\delta\omega-\delta\lambda) - (1-\delta\omega^2)\left(\delta\omega_0^2 - (\delta\omega-\delta\lambda)^2\right)}.$$

Assuming that $\Omega = \text{const} \Rightarrow \delta\lambda = 0$, we can obtain the amplitude and phase of the secondary oscillations when the angular rate is constant. By making the following substitutions

$$A_{11,12} = A_{20}(1 \pm \delta A), \qquad \varphi_{11,12} = \varphi_0 \pm \Delta\varphi,$$

solution (26) will be changed to

$$x_1(t) = 2A_{20}[\cos(\lambda t + \Delta\varphi)\sin(\omega t + \varphi_0) + \delta A \sin(\lambda t + \Delta\varphi)\cos(\omega t + \varphi_0)].$$

After multiplying the signal corresponding to the secondary oscillations on a phase shifted carrier signal $\sin(\omega t + \varphi_0)$, the output will be as follows

$$x_1^*(t) = A_{20}[\cos(\lambda t + \Delta\varphi) - \cos(\lambda t + \Delta\varphi)\cos(2\omega t + 2\varphi_0) + \delta A \sin(\lambda t + \Delta\varphi)\sin(2\omega t + 2\varphi_0)].$$

The first term $A_{20}\cos(\lambda t + \Delta\varphi)$ is the signal related to the angular rate. All other terms have doubled frequency and must to be removed by means of filtering after demodulation. Note that the output signal is distorted both in amplitude and phase. Phase distortion $\Delta\varphi$ is very predictable in a very wide range by means of obtained formulae. The amplitude error caused by the harmonic angular rate is determined as

$$\delta\Omega = \frac{A_{20} - A_0}{A_0} \approx D_\lambda \delta\lambda^2, \tag{27}$$

where

$$D_\lambda = \left\{\delta\omega^6(3g_2 - 2) + h\delta\omega_0^2\left[\delta\omega_0^4(2+g_2) - \delta\omega^4(5g_2 - 6)\right] + \delta\omega_0^4\delta\omega^2\left[4h^2(g_2-1) - 2 - 3g_2\right]\right\} / g_2\left[\left(\delta\omega_0^4 + \delta\omega^4 - 2\delta\omega_0^2\delta\omega^2 h\right)\right]^2,$$

$$h = 1 - 2\zeta_2^2, \qquad A_0 = A_{20}(\delta\lambda = 0).$$

Formula (27) gives only approximate results but for small values of the relative frequency of the angular rate ($\delta\lambda$ = 0–0.01) they are acceptable. The exact formula is more complicated and there is no reason to use it in this context. Graphs corresponding to both approximate and exact dependences are shown in figure 5 but there is no visually detectable difference between them in the given range. It is apparent that the dynamic error increases if the ratio between the natural frequencies approaches unity. In addition, it is possible to calculate a bandwidth if we assume an acceptable relative dynamic error $\delta\Omega_{max}$

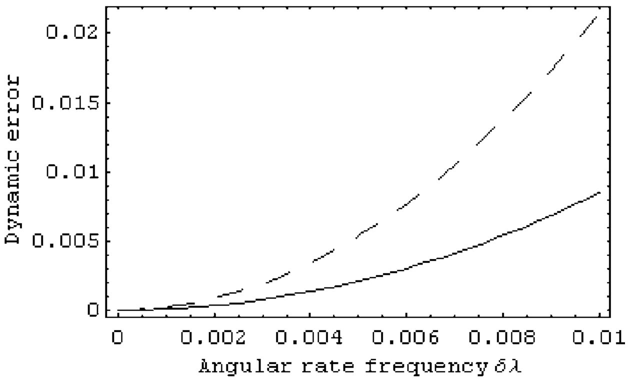

Figure 5. Dynamic error as a function of relative angular rate frequency: the dashed curve, $\delta\omega = 1.05$; the solid curve, $\delta\omega = 1.1$. The simulation data are: $\zeta_1 = \zeta_2 = 0.025$, $g_1 = 1$, $g_2 = 2$, $d_1 = d_2 = 1$, $q_1 = 10$ m s^{-2}, $\delta\omega_0 = 1$.

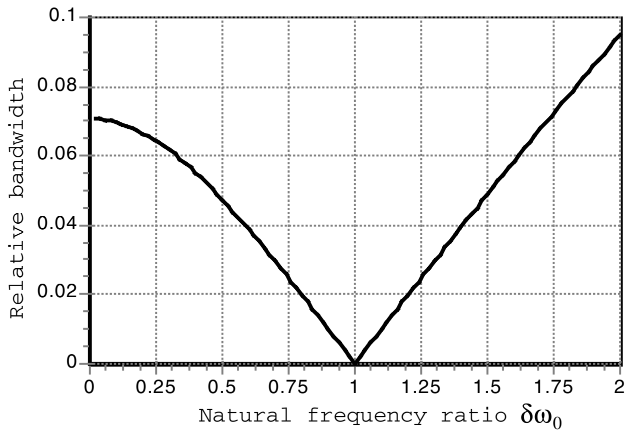

Figure 6. Relative bandwidth as a function of ratio of the natural frequencies. The simulation data are: $\delta\Omega_{max} = 0.01$, $\zeta_1 = \zeta_2 = 0.0001$, $g_1 = 1$, $g_2 = 2$, $d_1 = d_2 = 1$, $q_1 = 10$ m s^{-2}, $\delta\omega_0 = 1$.

$$B_\Omega = \omega_0\sqrt{\frac{\delta\Omega_{max}}{D_\lambda}}. \tag{28}$$

Here bandwidth B_Ω is measured in radians per second. The graph for the relative bandwidth (B_Ω/ω_0) is shown in figure 6.

Analysing both figures 6 and 2, we can see that, as the ratio of the natural frequencies approaches unity (i.e. $\delta\omega_0 \approx 1$), we obtain the maximal sensitivity but the minimal bandwidth. This effectively leads to a trade-off between these parameters. For open-loop gyroscopes, it is acceptable to have a ratio of natural frequencies in the range of 0.9–0.95. For the closed-loop operation, it is reasonable to have a ratio $\delta\omega_0 \approx 1$ for maximal sensitivity as well as providing required bandwidth by the feedback.

Due to inaccuracies of the present fabrication technologies, springs and other elements of the elastic suspension may have unknown and unpredictable deviations from the design values. This will result in deviations in the main parameters of the sensitive element. As shown above, one of the main parameters which is important for both sensitivity and bandwidth is the ratio of the natural frequencies. Let us consider small deviations of natural frequencies caused by the production inaccuracies. Deviations of natural frequencies will result in the deviation of the ratio of the natural frequencies as given by

$$\delta\omega_0^* = \delta\omega_0(1 + \varepsilon_{\delta\omega}). \tag{29}$$

Using equation (29), we can calculate the relative deviation of the bandwidth that can be represented as follows

$$\delta B_\Omega = (B_\Omega - B_{\Omega 0})/B_{\Omega 0}, \tag{30}$$

where $B_{\Omega 0}$ is the bandwidth corresponding to the absence of deviations ($\varepsilon_{\delta k} = 0$). For small deviations $\varepsilon_{\delta k}$, we can represent equation (30) by the following formula

$$\delta B_\Omega \approx \frac{D_{\varepsilon 1}}{D_{\varepsilon 2}} \varepsilon_{\delta\omega}, \tag{31}$$

where

$$\begin{aligned} D_{\varepsilon 1} = \delta\omega_0^2 \Big\{ & \left(\delta\omega^2 - \delta\omega_0^2\right)^3 \left[(g_2 + 2)\delta\omega_0^2 + (7g_2 - 2)\delta\omega^2\right] \\ & - 8\delta\omega_0^2\delta\omega^2\zeta_2^4 \left[(5g_2 - 2)\delta\omega_0^4 + (g_2 - 2)\delta\omega^2\right] \\ & + 2\left(\delta\omega_0^2 - \delta\omega^2\right)\zeta_2^2 \left[(g_2 + 2)\delta\omega_0^6 + 3(7g_2 - 2)\delta\omega_0^4\delta\omega^2 \right. \\ & \left. + 3(2 + g_2)\delta\omega_0^2\delta\omega^4 + (7g_2 - 2)\delta\omega^6\right] \Big\}, \\ D_{\varepsilon 2} = \Big[& \left(\delta\omega_0^2 - \delta\omega^2\right)^2 + 4\delta\omega_0^2\delta\omega^2\zeta_2^2 \Big] \Big\{ (2 - 3g_2)\delta\omega^6 \\ & + (5g_2 - 6)h\delta\omega_0^2\delta\omega^4 + (2 + g_2)\delta\omega_0^6 h \\ & + \delta\omega_0^4\delta\omega^2 \left[6 - g_2 + 16(g_2 - 1)\zeta_2^2 - 16(g_2 - 1)\zeta_2^4\right] \Big\}. \end{aligned}$$

Note that this relative deviation of the bandwidth does not depend on the absolute value of the driving frequency.

8. Design trade-offs

The presented analysis of the sensitivity, linearity and bandwidth have resulted in two design trade-offs. Firstly, in order to increase sensitivity, working frequency has to be as low as possible, but at the same time there is a lower limit that depends on scale factor linearity requirements. As a result, the natural frequency of the primary oscillations can be chosen by means of formula (11) taking into consideration the acceptable value of the nonlinearity and required measurement range. Secondly, in order to obtain maximum sensitivity, both natural frequencies of primary and secondary oscillations have to be of the same value, but this will result in a minimum for the bandwidth. This trade-off can be resolved by formula (28) so the ratio of the natural frequencies will have to be designed providing necessary bandwidth. As a result, parameters such as driving frequency, primary natural frequency (natural frequency of the primary oscillations) and ratio of the natural frequency can be directly calculated and they have to be precisely implemented during sensitive element design.

9. Conclusion

The presented analytical approach to the design of the sensitive element of micromechanical vibratory gyroscopes allows both prediction of the performances and determination of the dynamic parameters that are necessary to achieve high performance of inertial instruments. Even though the proposed approach is applied to sensitive elements, most of the dependences can also be used for detailed analysis of the dynamics of micromechanical gyroscopes while designing control circuits. Sensitivity to the angular rate was detected even without vacuum packaging and low-noise on-chip ASIC.

Acknowledgments

We would like to acknowledge the assistance of Mr Tang Xiaosong and Ms Chan Mei Lin in fabrication and testing of the gyroscope. VA is grateful to the Inertial Sensors and Control Systems of Flying Vehicles department of the Aero-Space Systems Faculty in the National Technical University of Ukraine ‘Kiev Polytechnic Institute’ and personally to Professor Alexander Zbrutsky for useful discussions during the earlier stages of this work.

References

[1] Friedland B and Hutton M F 1978 Theory and error analysis of vibrating-member gyroscope *IEEE Trans. Autom. Control* **23** 545–56

[2] Lynch D 1995 Vibratory gyro analysis by the method of averaging *Proc. 2nd St Petersburg Conf. on Gyroscopic Technology and Navigation (St Petersburg)* pp 26–34

[3] Shkel A M, Horowitz R, Seshia A and Howe R T 1999 Dynamics and control of micromachined gyroscopes *The American Control Conference (San Diego, CA)* pp 2119–24

[4] Shkel A M, Howe R T and Horowitz R 1999 Modeling and simulation of micromachined gyroscopes in presence of imperfections *Int. Conf. on Modeling and Simulation of Microsystems MSM'99 (Puerto Rico, USA)*

[5] Apostolyuk V and Zbrutsky A 1997 Investigation of micromechanical inertial devices *Proc. 4th St Petersburg Int. Conf. on Integrated Navigation Systems (St Petersburg)* pp 330–6

[6] Apostolyuk V and Zbrutsky A 1998 Research of dynamics of a gimballed micromechanical gyroscope *Scientific News of the National Technical University of Ukraine (Kiev)* no 3 pp 115–21

[7] Apostolyuk V and Zbrutsky A 2000 Thermal errors of gimballed micromechanical gyroscopes *Mechanics of Gyroscopic Systems (Kiev)* no 5–16 pp 3–10

[8] Apostolyuk V and Zbrutsky A 1998 Dynamics of a sensitive element of the micromechanical gyroscopes with an additional frame *Gyroscopes and Navigation (St Petersburg)* no 3 pp 13–23

[9] Apostolyuk V and Zbrutsky A 1999 Dynamics of a sensitive element of micromechanical gyroscope *Scientific News of the National Technical University of Ukraine (Kiev)* no 1 pp 114–20

[10] Geiger W, Folkmer B, Sobe U, Sandmaier H and Lang W 1998 New designs of micromachined vibrating rate gyroscopes with decoupled oscillation modes *Sensors Actuators* A **66** 118–24

[11] Apostolyuk V and Zbrutsky A 2000 Comparative analysis of the performances of micromechanical gyroscopes with translation and angular motions of sensitive elements *Gyroscopes and Navigation (St Petersburg)* no 1 pp 22–34

[12] Apostolyuk V and Zbrutsky A Sensitive element's structure optimisation for gimballed micromechanical gyroscopes *Mechanics of Gyroscopic Systems (Kiev)* no 5–16 pp 11–9